Pet. Sci. (2015) 12:518–524
DOI 10.1007/s12182-015-0034-9

ORIGINAL PAPER

Thermal decomposition characteristics and kinetics of methyl linoleate under nitrogen and oxygen atmospheres

Xue-Chun Wang[1] · Jian-Hua Fang[1] · Bo-Shui Chen[1] · Jiu Wang[1] · Jiang Wu[1] · Di Xia[1]

Received: 25 December 2014 / Published online: 22 July 2015

Abstract The thermal decomposition characteristics of methyl linoleate (ML) under nitrogen and oxygen atmospheres were investigated, using a thermogravimetric analyzer at a heating rate of 10 °C/min from room temperature to 600 °C. Furthermore, the pyrolytic and kinetic characteristics of ML at different heating rates were studied. The results showed that the thermal decomposition characteristics of ML under nitrogen and oxygen atmospheres were macroscopically similar, although ML exhibited relatively lower thermal stability under an oxygen atmosphere than under a nitrogen atmosphere. The initial decomposition temperature, the maximum weight loss temperature, the peak decomposition temperature, and the rate of maximum weight loss of ML under an oxygen atmosphere were much lower than those under a nitrogen atmosphere and increased with increasing heating rates under either oxygen or nitrogen atmosphere. In addition, the kinetic characteristics of thermal decomposition of ML were elucidated based on the experimental results and by the multiple linear regression method. The activation energy, pre-exponential factor, reaction order, and the kinetic equation for thermal decomposition of ML were obtained. The comparison of experimental and calculated data and the analysis of statistical errors of pyrolysis ratios demonstrated that the kinetic model was reliable for pyrolysis of ML with relative errors of about 1 %. Finally, the kinetic compensation effect between the pre-exponential factors and the activation energy in the pyrolysis of ML was also confirmed.

Keywords Methyl linoleate · Pyrolysis characteristics · Kinetics · Thermogravimetric analysis · Biodiesel

1 Introduction

With the decrease of petroleum reserves and the increase of environmental pollution brought by the extensive use of petroleum, alternative fuels and renewable resources have attracted increasing attention worldwide from the perspective of environmental protection and resource strategy (Lin et al. 2011; Demirbas 2009; Huang et al. 2012; Sharma and Singh 2009; Nigam and Singh 2011). Biodiesel, referred to as mixtures of fatty acid mono-alkyl esters with relatively high contents of long-chain, mono- and poly-unsaturated compounds, is produced from vegetable oils and animal fats by transesterification with alcohols of low molecular weights over catalysts (Candeia et al. 2009; Leung et al. 2010; Moser and Vaughn 2010). Fatty acid methyl esters (FAME) such as soybean methyl ester (SME) are typically mixtures of esters with 16-18 carbon atoms, where 80 %–85 % (w/w) of the mixture is unsaturated (Knothe et al. 2005). However, the presence of such mono- and poly-unsaturated compounds makes biodiesel extremely liable to thermal decomposition at elevated temperatures.

As we know, during the operation of a biodiesel-powered engine, small amounts of biodiesel will leak into the crankcase by oil seepage flow or gas entrainment. The leakage of biodiesel into the engine crankcase markedly lowers the quality of the engine oils due to thermal instability of biodiesel. At present, some studies have been

✉ Jian-Hua Fang
fangjianhua71225@sina.com

[1] Department of Military Oil Application & Administration Engineering, Logistical Engineering University, Chongqing 401311, China

Edited by Xiu-Qin Zhu

made on biodiesel-induced deterioration of engine oil for facilitating development and application of biodiesel as a clean and renewable petro-diesel substitute (Gili et al. 2011; Watson and Wong 2008; Wang et al. 2009). However, the thermal decomposition characteristics and kinetics of biodiesels, as well as their influences on deterioration of engine oils, have so far not been investigated intensively, partly because of the complexity of their pyrolytic chemical behavior and mechanisms. In fact, thermal instability of biodiesel is governed by its chemical nature, especially the structure and composition of unsaturated fatty acid methyl esters. It is therefore essential to investigate the thermal decomposition behavior of unsaturated FAME so as to better understand the nature of biodiesel-induced deterioration of engine oil. In this paper, the thermal decomposition characteristics and kinetics of unsaturated methyl linoleate were studied by thermogravimetric (TG) analysis. The present investigation is of importance for further understanding the pyrolytic behaviors of biodiesel and, in the nature of things, its influence on engine oil deterioration.

2 Experimental

2.1 Materials and apparatus

(1) Methyl linoleate (ML): an analytically purified chemical supplied by Xiya Reagent Research Center (China).
(2) TG analyzer: SDT-Q600 model, TA Instruments, USA.

2.2 TG analysis

The pyrolysis characteristics of ML were tested on the TG analyzer. In each test run, approximately 7 mg of ML was put uniformly on the bottom of an alumina crucible and the crucible was placed at the same position of the beam platform of the analyzer. Subsequently, the sample was progressively heated from room temperature to 600 °C at different heating rates of 10, 15, 20, and 30 °C/min under nitrogen or oxygen gas carrier flowing at 50 mL/min. The weight loss and heat flow changes in response to temperature were recorded. Finally, the TG and differential thermogravimetric (DTG) curves were plotted and the pyrolysis kinetics were studied.

3 Results and discussion

3.1 Pyrolysis characteristics of ML

Figure 1 shows the TG–DTG curves of ML at a heating rate of 10 °C/min. Table 1 shows the pyrolysis parameters of ML. From Fig. 1 and Table 1, it can be clearly observed that the thermal decomposition characteristics of ML under nitrogen and oxygen atmospheres were macroscopically similar. With increasing temperatures, the pyrolysis process in TG curves can be divided into three stages viz., the drying stage ($<T_s$), the main pyrolysis stage (T_s–T_f), and the residue decomposition stage ($>T_f$). The first stage occurred as the temperature increased from room temperature to the initial decomposition temperature T_s. In this

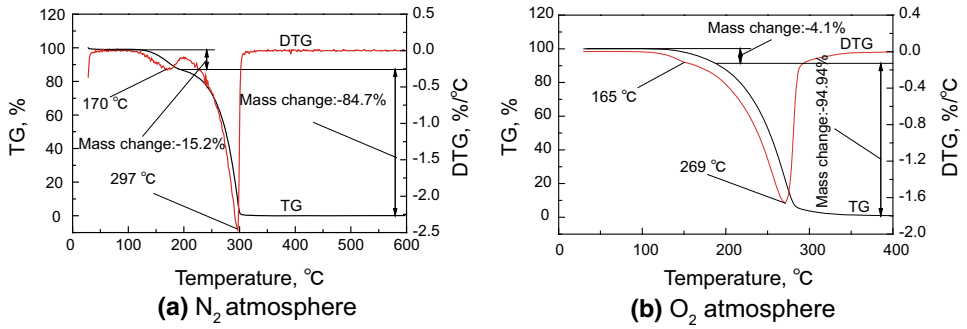

Fig. 1 TG/DTG curves of ML at different atmospheres ($\beta = 10$ °C/min)

Table 1 Pyrolysis parameters of ML at different atmospheres

Pyrolysis stage	N_2 atmosphere				O_2 atmosphere			
	Temperature range, °C	T_{max}, °C	$(dM/d\tau)_{max}$, %/°C	Mass loss, %	Temperature range, °C	T_{max}, °C	$(dM/d\tau)_{max}$, %/°C	Mass loss, %
Stage I	105–210	170	0.265	15.2	110–145	165	0.165	4.1
Stage II	210–300	297	2.47	84.7	145–285	269	1.65	94.9

T_{max}—peak temperature of DTG curve, °C; $(dM/d\tau)_{max}$—the maximum weight loss rate %/°C

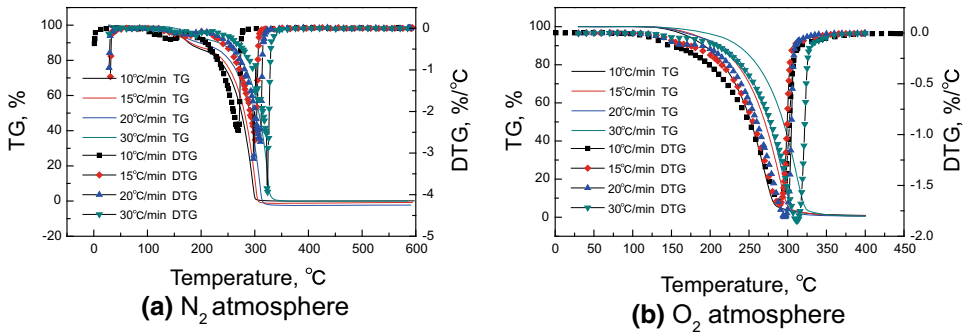

Fig. 2 TG/DTG curves of ML at different heating rates

Table 2 Pyrolysis parameters of ML at different heating rates

Pyrolysis stage	β, °C/min	N_2 atmosphere				O_2 atmosphere			
		Temperature range, °C	T_{max}, °C	$(dM/d\tau)_{max}$, %/°C	Mass loss, %	Temperature range, °C	T_{max}, °C	$(dM/d\tau)_{max}$, %/°C	Mass loss, %
Stage I	10	105–210	170	0.265	15.2	110–145	165	0.165	4.1
	15	115–225	192	0.279	13.5	115–160	167	0.169	3.9
	20	120–230	229	0.280	11.4	120–170	172	0.207	3.6
	30	120–230	238	0.286	9. 5	125–175	177	0.212	2.9
Stage II	10	210–300	297	2.47	84.7	145–285	269	1.65	94.9
	15	225–305	302	2.68	87.3	160–310	283	1.70	96.7
	20	230–310	310	3.14	90.9	170–315	287	1.81	96.7
	30	230–330	323	3.94	90.5	175–330	299	1.85	97.1

stage, a small weight loss could be observed due to evaporation of volatiles. The second stage occurred as the temperature increased from T_s to the maximum weight loss temperature T_f. The great weight loss in this stage was attributed to significant thermal decomposition of ML at elevated temperatures. The third stage occurred as the temperature increased from T_f to 600 °C; during the third stage almost no further weight loss could be detected. Figure 1 indicates that there were only two main weight loss stages in the TG curve, corresponding to two peaks in the DTG curve viz., the first stage ($<T_s$) and the second stage (T_s–T_f). However, it can also be observed from Fig. 1 and Table 1 that the pyrolysis characteristics of ML under nitrogen and oxygen atmospheres were slightly different. The peak temperature (T_{max}) and the initial decomposition temperature (T_s) of ML under an oxygen atmosphere were lower than those under nitrogen during the whole process, indicating that the thermal decomposition was easier under an oxygen atmosphere. Lower thermal stability of ML under oxygen might be attributed to a unique molecular structure containing two double bonds, thus enhancing decomposition of ML and promoting its thermal oxidation degradation at lower temperature (Wongsiriamnuay and Tippayawong 2010).

To further understand the pyrolysis characteristics of ML, thermogravimetric tests at different heating rates, i.e., 10, 15, 20, and 30 °C/min, were also conducted. The pyrolysis curves of ML at different heating rates are shown in Fig. 2. Also the main pyrolysis characteristics parameters of ML are shown in Table 2. It can be observed from the TG curves in Fig. 2 that the decomposition temperatures at different heating rates were slightly different. When the heating rate increased from 10 to 30 °C/min, the initial temperature of the main decomposition shifted to a higher one. Figure 2 shows the DTG profiles obtained from the thermal decomposition of ML at different heating rates. The maximum weight loss rate increased, and the corresponding peak temperature at maximum weight loss rate shifted to higher temperatures, with increasing heating rate. When the heating rate increased from 10 to 30 °C/min, the maximum weight loss rate sharply increased, and the peak of weight loss in the DTG curves became higher and broader. The increase of the initial decomposition temperature, the maximum weight loss temperature, the peak decomposition temperature, and of the maximum weight loss rate with increasing heating rates may be resulted from the reduction of the activation energy, as well as from the delay of

heat transfer during ML thermal decomposition (Park et al. 2009; Chen et al. 2011; Liang et al. 2014).

3.2 Kinetics of thermal decomposition of ML

3.2.1 Kinetic modeling

The kinetic parameters obtained from TG and DTG analysis are exceedingly crucial for efficient evaluation and calculation of the thermal decomposition process of ML. Assuming that the thermal decomposition of ML was a non-isothermal process, the decomposition rate equation can be given as follows:

$$\mathrm{d}\alpha/\mathrm{d}t = kf(\alpha)^n, \tag{1}$$

where α is the conversion rate and is defined as $\alpha = (m_0 - m_t)/(m_0 - m_\infty)$; m_0 is the initial weight of the test sample; m_t is the weight after a specified decomposition duration t; m_∞ is the weight of the indecomposable residue; n is the reaction order; and k is the reaction rate constant.

Generally, the Arrhenius equation is applicable in thermal decomposition reactions. Based on the Arrhenius equation, the reaction rate constant, k, for thermal decomposition of ML is given below:

$$k = A\exp(-E/RT), \tag{2}$$

where A is the pre-exponential factor, E is the activation energy (kJ/mol), T is the reaction temperature (K) and R is the ideal gas constant.

Since the mechanism function $f(\alpha)$ in Eq. (1) is dependent on the reaction model and reaction mechanism during pyrolysis process, for a simple reaction, $f(\alpha)$ is suggested as

$$f(\alpha) = (1-\alpha)^n. \tag{3}$$

Then, Eqs. (1), (2), and (3) can be combined to give

$$\mathrm{d}\alpha/\mathrm{d}t = A\exp(-E/RT)\,f(\alpha) = A\exp(-E/RT)(1-\alpha)^n. \tag{4}$$

Furthermore, substituting the heating rate, β, into Eq. (4) gives

$$\mathrm{d}\alpha/\mathrm{d}T = \frac{A}{\beta}\exp(-E/RT)(1-\alpha)^n, \tag{5}$$

where $\beta = \mathrm{d}T/\mathrm{d}t$ and $\mathrm{d}\alpha/\mathrm{d}T$ is the ratio of weight changes with temperature.

3.2.2 Determination of kinetic parameters

According to the kinetic model given above, the kinetic parameters such as pre-exponential factor, activation energy, and reaction order, and the most probable mechanism function for thermal decomposition of ML were determined by the multiple linear regression method.

Taking the natural logarithm of Eq. (5) gives

$$\ln(\mathrm{d}\alpha/\mathrm{d}T) = \ln\frac{A}{\beta} - E/RT + n\ln(1-\alpha). \tag{6}$$

Equation (6) may be further expressed in the linear form as given below:

$$Y = B + CX + DZ, \tag{7}$$

where $Y = \ln(\mathrm{d}\alpha/\mathrm{d}T)$, $X = 1/T$, $Z = \ln(1-\alpha)$, $B = \ln(A/\beta)$, and $C = -E/R$, $D = n$.

The constants B, C, and D were estimated by the multiple linear regression method with the TG–DTG data for pyrolysis of ML using Origin 8.0 software. The kinetic parameters viz., pre-exponential factor, activation energy, and reaction order, for each test run are presented in Table 3. The high correlation coefficients, R^2, shown in Table 3, demonstrated that the kinetic parameters calculated by the multiple linear regression method were reliable.

Table 3 Pyrolysis kinetic parameters of ML at different heating rates

Pyrolysis stage	β, °C/min	N_2 atmosphere					O_2 atmosphere				
		Temperature range, °C	Reaction order (n)	E, kJ/mol	$\ln A$	R^2	Temperature range, °C	Reaction order (n)	E, kJ/mol	$\ln A$	R^2
Stage I	10	105–210	36.8	105.25	33.08	0.970	110–145	28.7	103.14	25.44	0.999
	15	115–225	38.9	100.57	30.18	0.906	115–160	38.7	101.49	24.75	0.999
	20	120–230	47.3	98.62	28.53	0.924	120–170	39.5	95.22	23.53	0.999
	30	120–230	50.6	88.62	20.90	0.883	125–175	38.1	62.14	13.41	0.999
Stage II	10	210–300	0.160	83.14	21.31	0.992	145–285	0.437	49.87	9.54	0.970
	15	225–305	0.310	94.42	26.59	0.974	160–310	0.291	50.56	9.60	0.980
	20	230–310	0.200	95.08	26.90	0.982	170–315	0.278	54.26	10.59	0.975
	30	230–330	0.040	97.36	28.36	0.988	175–330	0.394	59.67	11.84	0.995

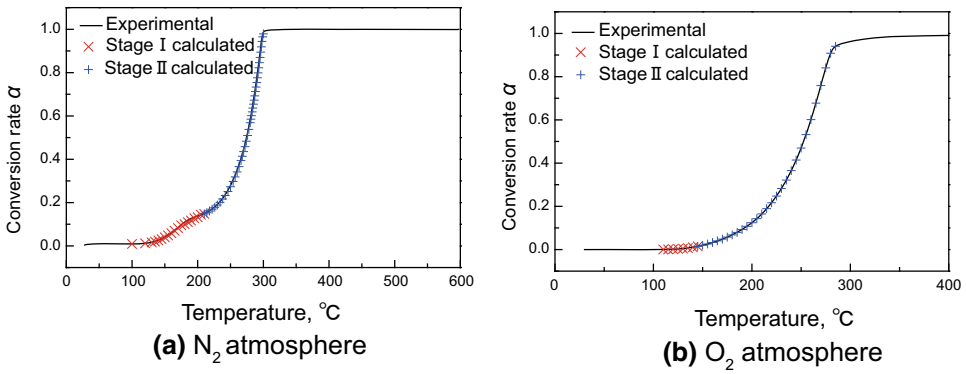

Fig. 3 Comparison of conversion rate between the experimental data and the calculated data by multiple linear regression

Table 4 Numerical statistical errors of conversion rate between the experimental data and the calculated data by multiple linear regression

Atmosphere	Reaction order (n)	Error, %	B, °C/min			
			10	15	20	30
N_2	–	RMSE	1.8793	2.4414	2.3718	2.5014
	–	MAPE	1.6402	1.9774	2.1897	2.0611
O_2	–	RMSE	3.1244	2.7745	2.7561	1.8252
	–	MAPE	2.2188	3.0143	3.1178	2.9112

3.2.3 *Kinetic reliability analysis*

The relationship and the numerical statistical errors of conversion rate between the experimental data and the calculated data by the multiple linear regression method at the heating rate of 10 °C/min are shown in Fig. 3 and Table 4, respectively. The numerical statistical errors of root mean square error (RMSE) and mean absolute percentage (MAPE) were calculated by the following equations:

$$\mathrm{RMSE} = \sqrt{\frac{1}{p}\sum_{i=1}^{p}(E_i - C_i)^2}$$

$$\mathrm{MAPE} = \sum_{i=1}^{p}\left|\frac{E_i - C_i}{E_i}\right| \times \frac{100}{p},$$

where p is the total number of observations considered in the test; E_i and C_i correspond to the experimental data and the calculated data of conversion rate, respectively.

It can be clearly observed from Fig. 3 and Table 4 that the experimental data and the calculated data of conversion rates obtained from the kinetic model by the multiple linear regression method are in good agreement, and the numerical statistical errors are not notable. This indicated that on one hand the suggested kinetic mechanism function, $f(\alpha) = (1-\alpha)^n$, fitted well with the pyrolysis kinetic regularity of ML and the kinetics modeling was thus reliable and on the other hand the multiple linear regression method was more available in the analysis of ML pyrolysis kinetics model.

3.2.4 *Kinetic compensation effect in pyrolysis of ML*

It has been found that for thermal decomposition reactions, the kinetic parameters, such as the pre-exponential factor A and the activation energy E, exhibit the following relationship (Cai and Bi 2009; Li et al. 2011):

$$\ln A = aE + b,$$

where a and b are constant coefficients. This relationship is referred to as the kinetic compensation effect, meaning that the pre-exponential factor of a thermal decomposition reaction is not a constant but changes with the variation of activation energy. Therefore, based on the kinetic parameters listed in Table 3, the relationship between $\ln A$ and E for pyrolysis of ML was plotted, as shown in Fig. 4. The kinetic parameters E and A were found to satisfy the kinetic compensation effect relationship, and their linear relationship is listed in Table 5. By comparison of the correlation coefficients ranging from 0.996 to 0.997, the good linear relationship between $\ln A$ and E demonstrated that the pre-exponential factor for thermal decomposition of ML was kinetically well compensated by activation energy.

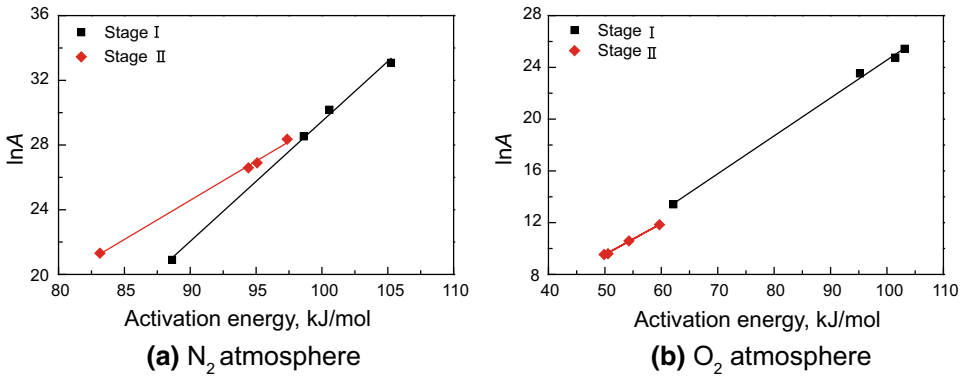

Fig. 4 Natural logarithm of pre-exponential factor against activation energy by MLR

Table 5 Relationship of kinetic compensation effects for ML at different atmospheres

Pyrolysis stage	N_2 atmosphere		O_2 atmosphere	
	Regression equation	R^2	Regression equation	R^2
Stage I	$\ln A_1 = 0.74116E_1 - 44.65774$	0.997	$\ln A_1 = 0.29309E_1 - 4.74191$	0.997
Stage II	$\ln A_2 = 0.48372E_2 - 18.95425$	0.996	$\ln A_2 = 0.23996E_2 - 2.47087$	0.997

4 Conclusions

The thermal decomposition characteristics of methyl linoleate under nitrogen and oxygen atmospheres were macroscopically similar. The initial decomposition temperature, the maximum weight loss temperature, and the peak decomposition temperature of methyl linoleate increased with increasing heating rates due to the increase of the activation energy and to the delay of heat transfer. However, the above-mentioned temperatures were much lower under an oxygen atmosphere, thus indicating that under oxygen methyl linoleate exhibited relatively poorer thermal stability. In addition, a kinetic model for thermal decomposition of methyl linoleate was built up, and the kinetic parameters such as activation energy, pre-exponential factor, and reaction order were obtained. The kinetic model was reliable in predicting the pyrolysis characteristics of methyl linoleate and provided a theoretical basis for expanding the experiment and anti-decomposition in biodiesel applications. Finally, the kinetic compensation effect between the pre-exponential factors and the activation energy in the pyrolysis of methyl linoleate was confirmed.

Acknowledgments The authors gratefully acknowledge the financial support provided by National Natural Science Foundation of China (Project No. 51375491) and the Natural Science Foundation of Chongqing (Project No. CSTC, 2014JCYJAA50021).

References

Cai JM, Bi LS. Kinetic analysis of wheat straw pyrolysis using isoconversional methods. J Therm Anal Calorim. 2009;98(1):325–30.

Candeia RA, Silva MCD, Carvalho Filho JR, et al. Influence of soybean biodiesel content on basic properties of biodiesel–diesel blends. Fuel. 2009;88(4):738–43.

Chen M, Qi X, Wang J, et al. Catalytic pyrolysis characteristics and kinetics of cotton stalk. J Fuel Chem Technol. 2011;39(8):585–9 (in Chinese).

Demirbas A. Progress and recent trends in biodiesel fuels. Energy Convers Manag. 2009;50(1):14–34.

Gili F, Igartua A, Luther R, et al. The impact of biofuels on engine oil's performance. Lubr Sci. 2011;23(7):313–30.

Huang D, Zhou H, Lin L. Biodiesel: an alternative to conventional fuel. Energy Procedia. 2012;16:1874–85.

Knothe G, Van Gerpen J, Krahl J. The biodiesel handbook. Champaign: AOCS Press; 2005.

Leung DYC, Wu X, Leung MKH. A review on biodiesel production using catalyzed transesterification. Appl Energy. 2010;87(4):1083–95.

Li D, Chen L, Zhang X, et al. Pyrolytic characteristics and kinetic studies of three kinds of red algae. Biomass Bioenergy. 2011;35(5):1765–72.

Liang Y, Cheng B, Si Y, et al. Thermal decomposition kinetics and characteristics of *Spartina alterniflora* via thermogravimetric analysis. Renew Energy. 2014;68:111–7.

Lin L, Cunshan Z, Vittayapadung S, et al. Opportunities and challenges for biodiesel fuel. Appl Energy. 2011;88(4):1020–31.

Moser BR, Vaughn SF. Coriander seed oil methyl esters as biodiesel fuel: unique fatty acid composition and excellent oxidative stability. Biomass Bioenergy. 2010;34(4):550–8.

Nigam PS, Singh A. Production of liquid biofuels from renewable resources. Prog Energy Combust Sci. 2011;37(1):52–68.
Park YH, Kim J, Kim SS, et al. Pyrolysis characteristics and kinetics of oak trees using thermogravimetric analyzer and micro-tubing reactor. Bioresour Technol. 2009;100(1):400–5.
Sharma YC, Singh B. Development of biodiesel: current scenario. Renew Sustain Energy Rev. 2009;13(6–7):1646–51.
Wang Z, Xu G, Huang H, et al. Reliability test of diesel engine fueled with biodiesel. Trans Chin Soc Agric Eng. 2009;25(11):169–72.
Watson SAG, VW Wong. The effects of fuel dilution with biodiesel and low sulfur diesel on lubricant acidity, oxidation and corrosion: a bench scale study with CJ-4 and CI-4+ lubricants[C]//STLE/ASME 2008 International Joint Tribology Conference. Am Soc Mech Eng. 2008;2008:233–5.
Wongsiriamnuay T, Tippayawong N. Thermogravimetric analysis of giant sensitive plants under air atmosphere. Bioresour Technol. 2010;101(23):9314–20.